Phase transitions in $MgSiO_3$ post-perovskite in super-Earth mantles

Koichiro Umemoto [a,b,c,*], Renata M. Wentzcovitch [d,e,f], Shunqing Wu [c,g], Min Ji [c], Cai-Zhuang Wang [c], Kai-Ming Ho [c]

[a] Earth-Life Science Institute, Tokyo Institute of Technology, Ookayama, Meguro-ku, Tokyo 152-8550, Japan
[b] Department of Earth Sciences, University of Minnesota, 310 Pillsbury drive SE, Minneapolis, MN 55455, USA
[c] Ames Laboratory, US DOE and Department of Physics and Astronomy, Iowa State University, Ames, IA 50011, USA
[d] Department of Applied Physics and Applied Mathematics, Columbia University, New York, NY 10027, USA
[e] Department of Earth and Environmental Sciences, Columbia University, New York, NY 10027, USA
[f] Lamont–Doherty Earth Observatory, Columbia University, Palisades, NY 10964, USA
[g] Department of Physics, Xiamen University, Xiamen 361005, China

a b s t r a c t

The highest pressure form of the major Earth-forming mantle silicate is $MgSiO_3$ post-perovskite (PPv). Understanding the fate of PPv at TPa pressures is the first step for understanding the mineralogy of super-Earths-type exoplanets, arguably the most interesting for their similarities with Earth. Modeling their internal structure requires knowledge of stable mineral phases, their properties under compression, and major element abundances. Several studies of PPv under extreme pressures support the notion that a sequence of pressure induced dissociation transitions produce the elementary oxides SiO_2 and MgO as the ultimate aggregation form at 3 TPa. However, none of these studies have addressed the problem of mantle composition, particularly major element abundances usually expressed in terms of three main variables, the Mg/Si and Fe/Si ratios and the Mg#, as in the Earth. Here we show that the critical compositional parameter, the Mg/Si ratio, whose value in the Earth's mantle is still debated, is a vital ingredient for modeling phase transitions and internal structure of super-Earth mantles. Specifically, we have identified new sequences of phase transformations, including new recombination reactions that depend decisively on this ratio. This is a new level of complexity that has not been previously addressed, but proves essential for modeling the nature and number of internal layers in these rocky mantles.

1. Introduction

The incredible 1995 discovery of a Jupiter mass planet around a sun-like star, Pegasi 51 (Mayor and Queloz, 1995), marked the dawn of a new age in planetary science and astronomy. Approximately 3,500 exoplanets have been confirmed since then, among which over 800 are super-Earths and nearly 400 are of terrestrial type, i.e., rocky planets. The discovery of these smaller rocky planets exploded with the deployment of the Kepler space telescope, which to date still has in its log $\approx$ 4,700 exoplanet candidates to be confirmed. Among these planets, the terrestrial ones are arguably the most interesting. Comparisons with Earth offer insights into our own planetary system formation process, and if found in the habitable zone, they might harbor life. Kepler 62e and 62f (Borucki et al., 2013), GJ 667c (Delfosse et al., 2013), Kepler 186f (Quintana et al., 2014), Kepler 438b and 442b (Torres et al., 2015), Wolf 1061c (Wright et al., 2016), and three planets in the TRAPPIST-1 system (Gillon et al., 2017) are remarkable examples of these potentially habitable planets. Super-Earths and mini-Neptunes with masses up to ~17 $M_\oplus$ are also remarkable because they seem to be relatively abundant, but none exist in our own solar system. These extraordinary discoveries are exciting public curiosity and interest and offer fertile grounds for frontier research. Planetary modelers have been actively studying super-Earths for over a decade (Valencia et al., 2006; Fortney et al., 2007; Seager et al., 2007; Sotin et al., 2007; Grasset et al., 2009; Bond et al., 2010; Sasselov and Valencia, 2010; Wagner et al., 2011; Dorn et al., 2015; Unterborn et al., 2016; Dorn et al., 2017; Unterborn and Panero, 2017). The general description of these planets' compositions and internal structures have been attained with knowledge of their masses, radii, and the basic equations governing the physics of planets, among which, the equation of state of planet forming materials is essential. Modern approaches to materials theory and simulations also started being employed a decade ago to investi-

gate the mineralogy of these planets (Umemoto et al., 2006). These calculations offer a level of detail that will be fundamental for understanding the dynamics of these planets. Mineral and aggregate phase diagrams, thermodynamics properties, and thermal conductivity are nowadays used as input for geodynamics simulations (Shahnas et al., 2011; Tosi et al., 2013) and will help answering questions regarding the nature of plate tectonics in these systems, a first order issue for habitability. These *ab initio* studies of materials properties at ultra-high pressures expand the horizons of materials simulations and offer targets for novel high pressure experimental techniques reaching nearly TPa pressures – a new frontier in high pressure research. In this paper we address the fate of $MgSiO_3$, the major Earth forming phase, up to 4 TPa from a new perspective. We focus on the important effect of the Mg/Si ratio of the lower mantle (Mg/Si_{LM}) as a key factor in determining phase equilibrium, therefore, the rocky mantle structure of super-Earths. $MgSiO_3$ perovskite (bridgmanite) is the major constituent of the Earth's mantle and its highest pressure polymorph in the mantle is post-perovskite (PPv) (Murakami et al., 2004; Oganov and Ono, 2004; Tsuchiya et al., 2004). In super-Earths, other forms of aggregation of MgO and SiO_2 stabilized by the higher pressures and temperatures in their mantles are expected. Several *ab initio* computational studies have predicted dissociations of $MgSiO_3$ PPv as post-PPv transitions (Umemoto et al., 2006; Umemoto and Wentzcovitch, 2011; Wu et al., 2014; Niu et al., 2015). These studies have shown that $MgSiO_3$ PPv should dissociate successively into $I\bar{4}2d$-type Mg_2SiO_4 + $P2_1/c$-type $MgSi_2O_5$, into Fe$_2$P-type SiO_2 + $I\bar{4}2d$-type Mg_2SiO_4, and then into the elementary oxides CsCl-type MgO + Fe$_2$P-type SiO_2 (see Supporting information for a brief explanation of the crystal structures). So far these post-PPv phase transitions have not been confirmed experimentally because of the extremely high pressures. In $MgSiO_3$ the Mg/Si ratio is 1, but the Earth's upper mantle – perhaps the whole mantle – has a Mg/Si ratio approximately equal to 1.25 and stars with orbiting planets have stellar Mg/Si ratios varying very widely (Adibekyan et al., 2015; Santos et al., 2015). Phase transitions and different aggregates may occur by varying Mg/Si_{LM} which impact the nature and number of internal layers in super-Earth mantles. In the present paper, we study these phase transitions in super-Earths with different Mg/Si_{LM} ratios using *ab initio* calculations combined with the adaptive genetic algorithm (AGA) (Ji et al., 2011; Wu et al., 2014) for structural search. We explore crystal structures with novel compositions in an unbiased manner without *a priori* assumptions of likely structural motifs.

2. Computational method

The AGA method employs auxiliary model potentials to enable fast exploration of structural space. With this efficient method we were able to investigate supercells with 2~8 formula units for all compounds considered here (up to 88 atoms). For more details of the AGA method, see Ji et al. (2011); Wu et al. (2014).

For first-principles calculations, we adopted the local-density approximation (Perdew and Zunger, 1981). To calculate total energies, forces and stresses during the AGA structural searches, we used the following pseudopotentials. For Mg, a pseudopotential by von Barth-Car's method (Karki et al., 2000). Five configurations, $3s^23p^0$, $3s^13p^1$, $3s^13p^{0.5}3d^{0.5}$, $3s^13p^{0.5}$, and $3s^13d^1$ with decreasing weights 1.5, 0.6, 0.3, 0.3, and 0.2, respectively, were used. Core radii for all quantum numbers l are 2.5 a.u.. The pseudopotentials for Si and O were generated by Vanderbilt's method (Vanderbilt, 1990). The valence electronic configurations used are $3s^23p^1$ and $2s^22p^4$ for Si and O. Core radii for all quantum numbers l are 1.6 and 1.4 a.u. for Si and O. The plane-wave cutoff energy is 40 Ry. Brillouin-zone integration was performed over **k**-point meshes of spacing $2\pi \times 0.05$ Å^{-1}. In order to refine

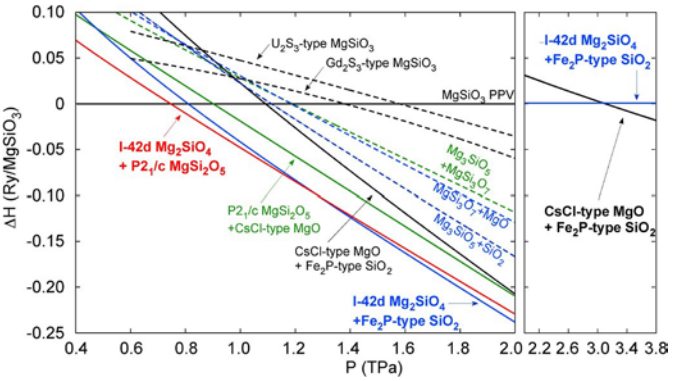

Fig. 1. Relative enthalpies of aggregation of possible dissociation products of $MgSiO_3$ and crystalline post-PPv $MgSiO_3$ with respect to $MgSiO_3$ PPv.

candidate structures obtained by the AGA searches, we used a set of harder pseudopotentials which are more suitable for ultrahigh pressures. They are the same as used in Umemoto et al. (2006); Umemoto and Wentzcovitch (2011). For these hard pseudopotentials, we used a cutoff energy of 400 Ry. Structural relaxations were performed using variable-cell-shape molecular dynamics (Wentzcovitch et al., 1993). To test for structural stability, phonon and vibrational density of states calculations were carried out for candidate structures using density-functional-perturbation theory (Baroni et al., 2001). We computed the vibrational contribution to the free energies within the quasiharmonic approximation (QHA) (Wallace, 1972). **k**-point grid for electronic-structure calculations and **q**-point grid for QHA were $(6 \times 6 \times 2, 12 \times 12 \times 10)$ for $MgSiO_3$ PPv, $(4 \times 4 \times 4, 12 \times 12 \times 12)$ for NaCl-type MgO, $(8 \times 8 \times 8, 16 \times 16 \times 16)$ for CsCl-type MgO, $(4 \times 4 \times 6, 16 \times 16 \times 16)$ for Fe$_2$P-type SiO_2, and $(4 \times 4 \times 4, 12 \times 12 \times 12)$ for $I\bar{4}2d$-type Mg_2SiO_4, and $(4 \times 2 \times 10, 8 \times 8 \times 8)$ for $P2_1/c$-type $MgSi_2O_5$. All first-principles calculations were performed using the Quantum-ESPRESSO (Giannozzi et al., 2009), which has been interfaced with the GA scheme in a fully parallel manner.

3. Results and discussion

3.1. Successive dissociations of $MgSiO_3$

As shown in previous studies (Wu et al., 2014; Niu et al., 2015), $MgSiO_3$ PPv undergoes successive dissociations: $MgSiO_3$ PPv → $I\bar{4}2d$-type Mg_2SiO_4 + $P2_1/c$-type $MgSi_2O_5$ at 0.75 TPa $I\bar{4}2d$-type Mg_2SiO_4 + Fe$_2$P-type SiO_2 (i.e., dissociation of $MgSi_2O_5$) at 1.31 TPa → CsCl-type MgO + Fe$_2$P-type SiO_2 at 3.10 TPa (see Fig. 1). It is worthwhile commenting on the crystal structure of $I\bar{4}2d$-type Mg_2SiO_4 (Fig. 2). For similar comments on $P2_1/c$-type $MgSi_2O_5$, see Umemoto and Wentzcovitch (2011). $I\bar{4}2d$-type Mg_2SiO_4 is a body-centered-tetragonal phase. As far as we know, this structure has not been identified in any other substance. However, its cation configuration is identical to that of Zn_2SiO_4-II whose space group is $I\bar{4}2d$ also (Marumo and Syono, 1971). The difference between $I\bar{4}2d$-type Mg_2SiO_4 and Zn_2SiO_4-II structures is in the oxygen sub-lattice. Both Mg and Si atoms are eight-fold coordinated, while Zn and Si atoms in Zn_2SiO_4-II are four-fold tetrahedrally coordinated. The structure of $I\bar{4}2d$-type Mg_2SiO_4 might be a viable high-pressure form of Zn_2SiO_4. Lattice dynamics calculations indicate that $I\bar{4}2d$-type Mg_2SiO_4 is dynamically stable at least up to 4 TPa. While Mg polyhedra share their faces, Si polyhedra share their edges. The eight-fold coordinated Mg and Si polyhedra are somewhat intermediate between NaCl-type octahedra and CsCl-type cubes. This type of cation site contrasts in $P2_1/c$-type $MgSi_2O_5$ where Mg and half of Si polyhedra form tricapped triangular prisms, which are structural units

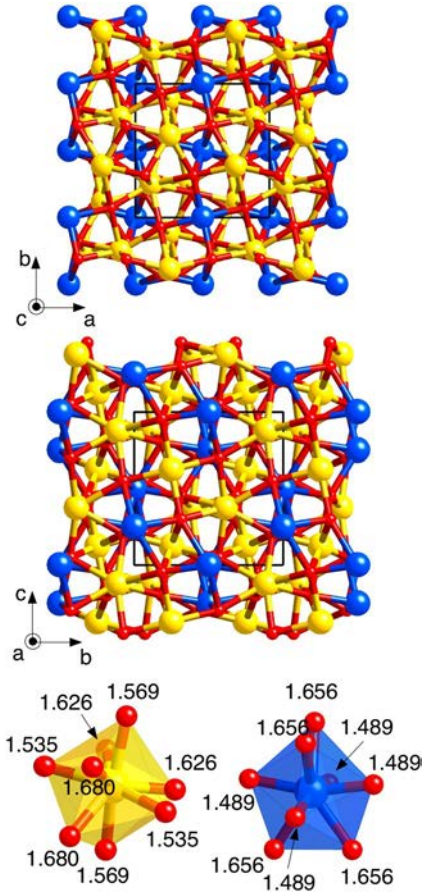

Fig. 2. Crystal structure of $I\bar{4}2d$-type Mg_2SiO_4. Yellow, blue, and red spheres denote Mg, Si and O atoms. Lattice constants at 1 TPa are $(a,\ c)$ (4.555 Å, 4.671Å). Atomic coordinates are Mg $(8d)$ (0.11348, 1/4, 1/8), Si $(4b)$ (0, 0, 1/2), and O $(16e)$ (0.93007, 0.81560, 0.79792). Bond lengths in Mg and Si polyhedra at 1 TPa are given in units of Å. (For interpretation of the references to color in this figure legend, the reader is referred to the web version of this article.)

of Fe_2P-type SiO_2 (Tsuchiya and Tsuchiya, 2011; Wu et al., 2011). The other half of Si sites are octahedrally coordinated with one extra oxygen attached. This is similar to the case of pyrite-type SiO_2. Thermodynamic quantities of $I\bar{4}2d$-type Mg_2SiO_4 obtained using the quasiharmonic approximation (QHA) are shown in Table S1; similar quantities for $P\,2_1/c$-type $MgSi_2O_5$ were published in a previous study (Umemoto and Wentzcovitch, 2011).

This dissociation of $MgSiO_3$ into Mg_2SiO_4, a MgO-rich compound, and $MgSi_2O_5$, a SiO_2-rich one, suggests the possibility of further dissociations into other MgO- and SiO_2-"richer" compounds, i.e., $(MgO)_m(SiO_2)$ with $m \geq 3$ and $(MgO)(SiO_2)_n$ with $n \geq 3$. To check this possibility, we performed structural searches for Mg_3SiO_5 ($m \geq 3$) and $MgSi_3O_7$ ($n \geq 3$) with the AGA. The lowest-enthalpy structures of Mg_3SiO_5 and $MgSi_3O_7$ are monoclinic with Cm and Pc symmetries, respectively (see Fig. 3). As shown in Fig. 1, this aggregate of Mg_3SiO_5 and $MgSi_3O_7$ is metastable with respect to that of Mg_2SiO_4 and $MgSi_2O_5$. The possibility of other higher pressure forms of $MgSiO_3$ was also investigate with the AGA. The lowest-enthalpy crystalline post-PPv phase of $MgSiO_3$ has Gd_2S_3-type structure (Fig. 3). The Gd_2S_3-type phase is a typical high-pressure structure in A_2O_3 type compounds (*e.g.* Umemoto and Wentzcovitch, 2010 and references therein). Gd_2S_3-type $MgSiO_3$ has lower enthalpy than U_2S_3-type, which was predicted to be the stable form of Al_2O_3 at ultra-high pressures (Umemoto and Wentzcovitch, 2008). Gd_2S_3-type $MgSiO_3$ is also metastable compared to the aggregate of Mg_2SiO_4 and $MgSi_2O_5$ (Fig. 1). Therefore, we exclude the possibilities of reactions involving $(MgO)_m(SiO_2)$ with $m \geq 3$, $(MgO)(SiO_2)_n$ with $n \geq 3$, and crystalline post-PPv $MgSiO_3$. We conclude that the vital compounds relevant to interiors of super-Earths are MgO, SiO_2, $MgSi_2O_5$, and Mg_2SiO_4.

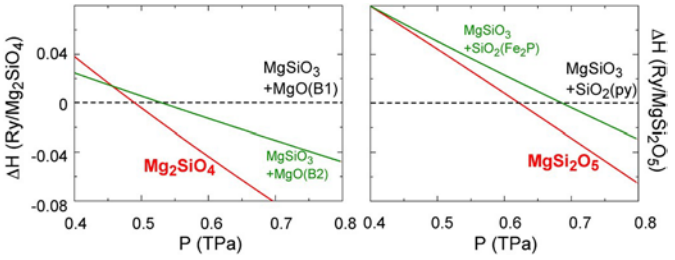

Fig. 4. Relative enthalpies of $I\bar{4}2d$-type Mg_2SiO_4 with respect to aggregations of $MgSiO_3$ and MgO (left) and $P\,2_1/c$-type $MgSi_2O_5$ with respect to aggregations of $MgSiO_3$ and SiO_2 (right).

3.2. Recombination of $MgSiO_3$ with MgO or SiO_2

Now we discuss the cases where $MgSiO_3$ PPv coexists with MgO or with SiO_2, which is expected in mantles with Mg/Si_{LM} ratio > 1 and < 1, respectively. The low-pressure form of MgO, NaCl-type, transforms to the CsCl-type phase (Coppari et al., 2013). The static transition pressure of 0.53 TPa is consistent among *ab initio* calculations (*e.g.* Mehl et al. (1988)). QHA free energy calculations indicate that NaCl-type MgO and $MgSiO_3$ PPv combine to form $I\bar{4}2d$-type Mg_2SiO_4 beyond 0.49 TPa (see Fig. 4(left)). This is surprising because in the Earth Mg_2SiO_4 ringwoodite, a major transition zone phase, dissociates into MgO periclase and $MgSiO_3$ bridgmanite. In the Earth's mantle these phases contain small amounts of Fe, but the dissociation also exists in the Fe-free compound. This dissociation transition is responsible for the major "660 km" velocity discontinuity defining the upper boundary of the lower mantle. Here we see that under much higher pressures corresponding to the deep interiors of super-Earths, NaCl-type MgO and $MgSiO_3$ PPv recombine into $I\bar{4}2d$-type Mg_2SiO_4. Similarly, $MgSiO_3$ PPv and pyrite-type SiO_2 combined into $P\,2_1/c$-type $MgSi_2O_5$ at 0.62 TPa (see Fig. 4(right)). These recombination pressures are

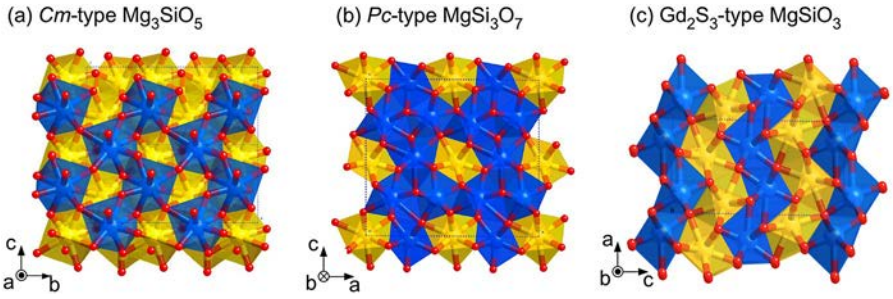

Fig. 3. Crystal structures of (a) Cm-type Mg_3SiO_5, (b) Pc-type $MgSi_3O_7$ and (c) Gd_2S_3-type $MgSiO_3$. Structural parameters are given in Table S2.

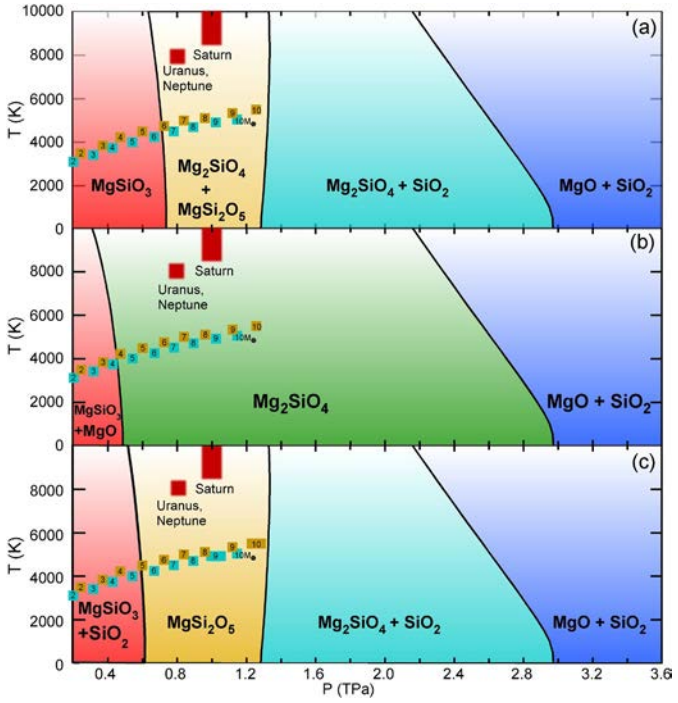

Fig. 5. Phase diagram showing (a) three-stage of dissociations of $MgSiO_3$ PPv, (b) recombination of $MgSiO_3$ PPv and NaCl-type MgO, and (c) recombination of $MgSiO_3$ and pyrite-type SiO_2; in (b) and (c), the molar ratios between $MgSiO_3$ and MgO/SiO_2 are 1:1. Red spots denote estimated pressure-temperature conditions at core-envelope boundaries in the solar giants (Jupiter's condition, ~4 TPa and ~15,000–20,000 K, is not shown here) (Guillot, 2004). Brown and light blue squares represent pressure-temperature conditions at CMB in terrestrial and ocean exoplanets, assuming their Earth-like chemical compositions[1] (Sotin et al., 2007). Numbers in squares indicate planet masses in units of Earth mass ($M_\oplus$). (For interpretation of the references to color in this figure legend, the reader is referred to the web version of this article.)

lower than the dissociation pressure of $MgSiO_3$ PPv into Mg_2SiO_4 and $MgSi_2O_5$ and also lower than the transition pressures of NaCl-type to CsCl-type MgO and of pyrite-type to Fe_2P-type SiO_2. A new view of super-Earth mantles then emerges.

4. Dissociation and recombination in super-Earths

The resulting sequence of phase transitions can be examined by computing aggregate phase diagrams using the QHA. For pure $MgSiO_3$, the sequence of dissociations predicted by static calculations (Wu et al., 2014) holds up to 10,000 K (see Fig. 5(a)). This result contrasts with a recent prediction (Niu et al., 2015) showing that a different sequence of dissociation reactions, namely $Mg_2SiO_4 + MgSi_2O_5 \rightarrow 3/2\ (MgSi_2O_5 + MgO)$ occurs above ~ 6,000 K. For super-Earths and ocean exoplanets with masses of 1–10 $M_\oplus$, CMB pressures and temperatures have been estimated assuming Earth-like mantle compositions and more basic thermal equations of state (Valencia et al., 2006; Sotin et al., 2007).[1] For mantles with

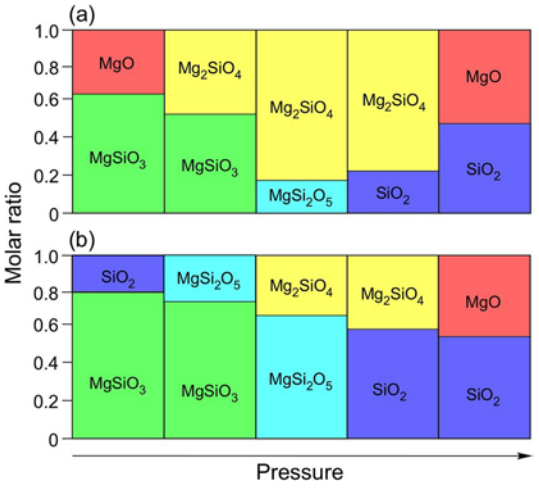

Fig. 6. Pressure-induced changes of molar ratio of components of super-Earth's mantle under pressure. (a) In a case of coexistence of $MgSiO_3$ and MgO. The molar ratio of $MgSiO_3$ and MgO is assumed to be 0.65:0.35, corresponding to $Mg/Si_{LM} = 1.54$. (b) In a case of coexistence of $MgSiO_3$ and SiO_2. The molar ratio of $MgSiO_3$ and SiO_2 is assumed to be 0.80:0.20, corresponding to $Mg/Si_{LM} = 0.8$.

Mg/Si ratio equal to 1, $MgSiO_3$ PPv survives in terrestrial and ocean super-Earths with masses smaller than $\sim 6M_\oplus$. In the presence of MgO the recombination of $MgSiO_3$ and MgO occurs when their masses are larger than $4M_\oplus$ (see Fig. 5(b)) while in the presence of SiO_2 the recombination transition is expected in planets with masses larger than $5M_\oplus$ (see Fig. 5(c)). The first dissociation into Mg_2SiO_4 and $MgSi_2O_5$ should occur in super-Earths with masses larger than $6M_\oplus$ for example Kepler-20b (Gautier et al., 2012) and possibly CoRoT-7b whose mass has been under debate (Leger et al., 2009; Hatzes et al., 2011). The Clapeyron slopes (slope of the phase boundary which is given by dP/dT on the phase boundary) of three successive dissociations in $MgSiO_3$ at 5,000 K (see Fig. 5(a)) are −10, +6, and −92 MPa/K, respectively. Those of the two recombination transitions, i.e., $MgSiO_3 + MgO \rightarrow Mg_2SiO_4$ and $MgSiO_3 + SiO_2 \rightarrow MgSi_2O_5$ are 16 and 9 MPa/K, respectively. Except for the dissociation of $MgSi_2O_5 \rightarrow Mg_2SiO_4 + SiO_2$ (Fig. 5(a) and (c)), the Clapeyron slopes of all phase boundaries are negative. Recombination and dissociation with large negative Clapeyron slopes in the middle of a silicate mantle may promote compositional layering (Christensen and Yuen, 1985; Peltier and Solheim, 1992; Tackley, 1995). In Mars, the post-spinel transition with negative Clapeyron slope near the CMB is believed to be the cause of a proposed large superplume (Weinstein, 1995). Similarly, in super-Earths with masses ~ $4M_\oplus$ (or ~ $6M_\oplus$), recombination of NaCl-type MgO and $MgSiO_3$ (or dissociation of $MgSiO_3$) could induce a comparable phenomenon.

Stellar Mg/Si ratios can vary substantially around 1 (Adibekyan et al., 2015; Santos et al., 2015) and the number of transitions up to 3 TPa increases in both Mg-rich and Si-rich mantles, in which $MgSiO_3$ coexists with MgO and SiO_2 respectively, because of the newly found recombination reactions. For Mg-rich mantles, by assuming the molar ratio between $MgSiO_3$ PPv and MgO to be $x : y\ (= 1/(Mg/Si_{LM} - 1))$, the sequence of transitions is as follows (Fig. 6(a)):

$$x\mathrm{MgSiO_3} + y\mathrm{MgO} \rightarrow (x-y)\mathrm{MgSiO_3} + y\mathrm{Mg_2SiO_4} \rightarrow \frac{x+2y}{3}\mathrm{Mg_2SiO_4} + \frac{x-y}{3}\mathrm{MgSi_2O_5}$$

[1] Mantle compositions and the size of core can be in first order specified by the relative abundances of Mg, Si, and Fe. Sotin et al. (2007) estimated pressure and temperature profiles in super-Earths by assuming Earth-like chemical compositions and equations of states of silicates in the mantle and iron alloys in the core; Mg/Si = 1.131, Fe/Si = 0.986, and Mg# = 0.9. Here we invoke CMB pressures and temperatures in super-Earths as reported in Sotin et al. (2007) as reference for the discussion on the effect of dissociation and recombination reactions in the mantle of these planets. However, it should be noted here that, if super-Earths have chemical compositions rather different from the Earth, their CMB pressures and temperatures should be different from those estimated in Sotin et al. (2007). A mass-radius relation study for 65 exoplanets showed that average density of exoplanets increases when their radii (R_P) are smaller than 1.5 Earth's radius ($R_\oplus$) but decreases when 1.5 $R_\oplus < R_P < 4R_\oplus$ (Weiss and Marcy, 2014); it suggests that chemical compositions of super-Earths with different radii may be different from those of the Earth.

$$\rightarrow \frac{x+y}{2}\,Mg_2SiO_4 + \frac{x-y}{2}\,SiO_2$$
$$\rightarrow (x+y)MgO + xSiO_2.$$

It should be noted that NaCl-type MgO disappears with the recombination transition and MgO emerges again in the CsCl-type form with the last dissociation transition. Earth-like mantle compositions possibly vary from pyrolitic (McDonough and Sun, 1995; Jackson, 1998; da Silva et al., 2000; Karki et al., 2001; Wentzcovitch et al., 2004; Irifune et al., 2010; Wang et al., 2015) to near-chondritic (Murakami et al., 2012). In a pyrolitic mantle $x : y \approx 0.65 : 0.35$ (if Fe is replaced by Mg, Ca by Mg, and Al by a (Mg,Si) coupled substitution). In this case, 67% $MgSiO_3$ PPv combines with NaCl-type MgO into Mg_2SiO_4, while 33% $MgSiO_3$ PPv survives and MgO disappears; therefore, the transition between NaCl- and CsCl-type MgO should not occur in super-Earths. The resulting molar fractions of $MgSiO_3$ and Mg_2SiO_4 are 0.46 and 0.54, respectively. After the first dissociation the molar fractions of Mg_2SiO_4 and $MgSi_2O_5$ are 0.82 and 0.18. For a near-chondritic mantle, the molar fractions of $MgSiO_3$ and MgO are $\sim$0.95 and 0.05. After the recombination the molar fractions of Mg_2SiO_4 and $MgSiO_3$ are 0.053 and 0.947, respectively, and after the first dissociation, the molar fractions of Mg_2SiO_4 and $MgSi_2O_5$ are 0.538 and 0.462. For Si-rich mantles, where $MgSiO_3$ PPv coexists with pyrite-type SiO_2. By assuming the molar ratio between $MgSiO_3$ PPv and SiO_2 to be $x : y(=1/(\mathrm{Si/Mg_{LM}} - 1))$, the transitions are (Fig. 6(b)):

$$xMgSiO_3 + ySiO_2 \rightarrow (x-y)MgSiO_3 + yMgSi_2O_5$$
$$\rightarrow \frac{x-y}{3}\,Mg_2SiO_4 + \frac{x+2y}{3}\,MgSi_2O_5$$
$$\rightarrow \frac{x}{2}\,Mg_2SiO_4 + \frac{x+2y}{2}\,SiO_2$$
$$\rightarrow xMgO + (x+y)SiO_2.$$

Pyrite-type SiO_2 disappears after the recombination and SiO_2 emerges again in the Fe_2P-type phase after the second dissociation. In overall, these recombination reactions produce one extra mantle layer (see Fig. 5) whose contrast in properties depend on how much $\mathrm{Mg/Si_{LM}}$ departs from 1.

5. Summary

This *ab initio* study addressing the stability of $MgSiO_3$ PPv in super-Earth mantles with Mg/Si ratios of the lower mantle different from 1 identified new recombination reactions in both Mg- and Si-rich mantles in addition to the previously reported dissociation reactions. These recombinations with negative Clapeyron slopes introduce an extra layer in the mantles of super-Earths with masses larger than $\sim 4M_\oplus$ if Mg-rich or $\sim 5M_\oplus$ if Si-rich. Structural searches using the adaptive genetic algorithm revealed that dissociations of $MgSiO_3$ into products such as $(MgO)_m(SiO_2)$ and $(MgO)(SiO_2)_n$ should not be expected and the relevant phases are those previously identified. Because of the recombination reaction, the NaCl- to CsCl-type transition in MgO does not occur in super-Earth mantles. CsCl-type MgO appears only with the final break down of Mg_2SiO_4 into pure oxides at much higher pressures and temperatures unlikely to materialize in mantles of super-Earths and mini-Neptunes. The last solid–solid transition identified so far remains the dissociation of Mg_2SiO_4 into the pure oxides Fe_2P-type SiO_2 and CsCl-type MgO at 3 TPa at low temperatures. This state of aggregation is the relevant one for the core of Jupiter like planets. Phase boundaries and thermodynamic quantities reported here should be important for modeling super-Earth interiors. Thermal conductivity is another important quantity for modeling super-Earth interiors, related to possibility of geodynamo and therefore implications for the habitability. First principles calculation of thermal conductivity should be performed, based on phase transitions we studied.

Although mantles of rocky planets more massive than Earth are expected to have achieved larger temperatures during formation, have ex-solved more Fe, and therefore are expected to have larger Mg# (= [Mg]/[Mg + Fe]) than the Earth's mantle, searches for silicate and oxide mineral phases with Fe_nO_m components should be undertaken in the future for a better understanding of these planets.

Acknowledgements

KU and RMW were supported by grants NSF/EAR 1047629, 1319368, and 1348066. KU is the main contributor to phonon and quasiharmonic computations using facilities at the Minnesota Supercomputing Institute and at the Laboratory for Computational Science and Engineering at the University of Minnesota and the ELSI supercomputing system at Tokyo Institute of Technology. SQW is the main contributor to the GA structure search performed at Ames Laboratory and SQW also acknowledges financial support from the National Natural Science Foundation of China (No. 11004165). Work at Ames Laboratory (KU, SQW, JM, CZW and KMH) was supported by the U.S. Department of Energy, Office of Science, Basic Energy Sciences, Materials Science and Engineering Division, including a grant of computer time at the National Energy Research Scientific Computing Centre (NERSC) in Berkeley, CA. Ames Laboratory is operated for the U.S. DOE by Iowa State University under contact number DE-AC02-07CH11358.

References

Adibekyan, V., Santos, N.C., Figueira, P., Dorn, C., Sousa, S.G., Delgado-Mena, E., Israelian, G., Hakobyan, A.A., Mordasini, C., 2015. From stellar to planetary composition: galactic chemical evolution of Mg/Si mineralogical ratio. Astron. Astrophys. 581, L2.

Baroni, S., de Gironcoli, S., Dal Corso, A., Giannozzi, P., 2001. Phonons and related crystal properties from density-functional perturbation theory. Rev. Mod. Phys. 73, 515–562.

Bond, J.C., O'Brien, D.P., Lauretta, D.S., 2010. The compositional diversity of extrasolar terrestrial planets. I. In situ simulations. Astrophys. J. 715, 1050–1070.

Borucki, W.J., et al., 2013. Kepler-62: a five-planet system with planets of 1.4 and 1.6 Earth radii in the habitable zone. Science 340, 587–590.

Christensen, U.R., Yuen, D.A., 1985. Layered convection induced by phase transitions. J. Geophys. Res. 90, 10291–10300.

Coppari, F., et al., 2013. Experimental evidence for a phase transition in magnesium oxide at exoplanet pressures. Nat. Geosci. 6, 926.

da Silva, C.R.S., Wentzcovitch, R.M., Patel, A., Price, G.D., Karato, S., 2000. The composition and geotherm of the lower mantle: constraints from the elasticity of silicate perovskite. Phys. Earth Planet. Inter. 118, 103.

Delfosse, X., et al., 2013. The HARPS search for southern extra-solar planets XXXIII. Super-Earths around the M-dwarf neighbors Gl 433 and Gl 667C. Astron. Astrophys. 553, A8.

Dorn, C., Hinkel, N.R., Venturini, J., 2017. Bayesian analysis of interiors of HD 219134b, Kepler-10b, Kepler-93b, CoRoT-7b, 55 Cnc e, and HD 97658b using stellar abundance proxies. Astron. Astrophys. 597, A38.

Dorn, C., Khan, A., Heng, K., Connolly, J.A.D., Alibert, Y., Benz, W., Tackley, P., 2015. Can we constrain the interior structure of rocky exoplanets from mass and radius measurements? Astron. Astrophys. 577, A83.

Fortney, J.J., Marley, M.S., Barnes, J.W., 2007. Planetary radii across five orders of magnitude in mass and stellar insolation: application to transits. Astrophys. J. 659, 1661–1672.

Gautier III, T.N., et al., 2012. Kepler-20: a sun-like star with three sub-Neptune exoplanets and two Earth-size candidates. Astrophys. J. 749, 15.

Giannozzi, P., et al., 2009. QUANTUM ESPRESSO: a modular and open-source software project for quantum simulations of materials. J. Phys. Condens. Matter 21, 395502.

Gillon, M., et al., 2017. Seven temperate terrestrial planets around the nearby ultra-cool dwarf star TRAPPIST-1. Nature 542, 456.

Grasset, O., Schneider, J., Sotin, C., 2009. A study of the accuracy of mass-radius relationships for silicate-rich and ice-rich planets up to 100 Earth masses. Astrophys. J. 693, 722–733.

Guillot, T., 2004. Probing the giant planets. Phys. Today 57, 63.

Hatzes, A.P., et al., 2011. The mass of CoRoT-7b. Astrophys. J. 743, 75.

Irifune, T., Shinmei, T., McCammon, C.A., Miyajima, N., Rubie, D.C., Frost, D.J., 2010. Iron partitioning and density changes of pyrolite in Earth's lower mantle. Nature 327, 193.

Jackson, I., 1998. Elasticity, composition and temperature of the Earth's lower mantle: a reappraisal. Geophys. J. Int. 134, 291.

Ji, M., Umemoto, K., Wang, C.Z., Ho, K.M., Wentzcovitch, R.M., 2011. Ultrahigh-pressure phases of H_2O ice predicted using an adaptive genetic algorithm. Phys. Rev. B 84. 220105(R).

Karki, B.B., Wentzcovitch, R.M., de Gironcoli, S., Baroni, S., 2000. High-pressure lattice dynamics and thermoelasticity of MgO. Phys. Rev. B 61, 8793–8800.

Karki, B.B., Wentzcovitch, R.M., de Gironcoli, S., Baroni, S., 2001. First principles thermoelasticity of $MgSiO_3$-perovskite: consequences for the inferred properties of the lower mantle. Geophys. Res. Lett. 28 (14), 2699–2702.

Leger, A., et al., 2009. Transiting exoplanets from the CoRoT space mission VIII. CoRoT-7b: the first super-Earth with measured radius. Astron. Astrophys. 506, 287–302.

Marumo, F., Syono, Y., 1971. The crystal structure of Zn_2SiO_4-II, a high-pressure phase of willemite. Acta Crystallogr., Sect. B 27, 1868–1870.

Mayor, M., Queloz, D., 1995. A Jupiter-mass companion to a solar-type star. Nature 378, 355.

McDonough, W.F., Sun, S.-s., 1995. The composition of the Earth. Chem. Geol. 120, 223–253.

Mehl, M.J., Cohen, R.E., Krakauer, H., 1988. Linearized augmented plane wave electronic structure calculations for MgO and CaO. J. Geophys. Res. 93, B8009–B8022.

Murakami, M., Hirose, K., Kawamura, K., Sata, N., Ohishi, Y., 2004. Post-perovskite phase transition in $MgSiO_3$. Science 304, 855–858.

Murakami, M., Ohishi, Y., Hirao, N., Hirose, K., 2012. A perovskitic lower mantle inferred from high-pressure, high-temperature sound velocity data. Nature 485, 90.

Niu, H., Oganov, A.R., Chen, X.Q., Li, D., 2015. Prediction of novel stable compounds in the Mg–Si–O system under exoplanet pressures. Sci. Rep. 5, 18347.

Oganov, A.R., Ono, S., 2004. Theoretical and experimental evidence for a post-perovskite phase of $MgSiO_3$ in Earth's D" layer. Nature 430, 445–448.

Peltier, W.R., Solheim, L.P., 1992. Mantle phase transitions and layered chaotic convection. Geophys. Res. Lett. 19, 321–324.

Perdew, J.P., Zunger, A., 1981. Self-interaction correction to density-functional approximations for many-electron systems. Phys. Rev. B 23, 5048–5079.

Quintana, E.V., et al., 2014. An Earth-sized planet in the habitable zone of a cool star. Science 344, 277–280.

Santos, N.C., Adibekyan, V., Mordasini, C., Benz, W., Delgado-Mena, E., Dorn, C., Buchhave, L., Figueira, P., Mortier, A., Pepe, F., Santerne, A., Sousa, S.G., Udry, S., 2015. Constraining planet structure from stellar chemistry: the cases of CoRoT-7, Kepler-10, and Kepler-93. Astron. Astrophys. 580, L13.

Sasselov, D.D., Valencia, D., 2010. Planets we could call home. Sci. Am. 303, 38–45.

Seager, S., Kuchner, M., Hier-Majumder, C.A., Militzer, B., 2007. Mass-radius relationships for solid exoplanets. Astrophys. J. 669, 1279–1297.

Shahnas, M.H., Peltier, W.R., Wu, Z., Wentzcovitch, R.M., 2011. The high-pressure electronic spin transition in iron: potential impacts upon mantle mixing. J. Geophys. Res. 116, B08205.

Sotin, C., Grasset, O., Mocquet, A., 2007. Mass-radius for extrasolar Earth-like planets and ocean planets. Icarus 191, 337–351.

Tackley, P.J., 1995. On the penetration of an endothermic phase transition by upwellings and downwellings. J. Geophys. Res. 100, 15477–15488.

Torres, G., et al., 2015. Validation of 12 small Kepler transiting planets in the habitable zone. Astrophys. J. 800, 99.

Tosi, N., Yuen, D.A., de Koker, N., Wentzcovitch, R.M., 2013. Mantle dynamics with pressure- and temperature-dependent thermal expansivity and conductivity. Phys. Earth Planet. Inter. 217, 48–58.

Tsuchiya, T., Tsuchiya, J., 2011. Prediction of a hexagonal SiO_2 phase affecting stabilities of $MgSiO_3$ and $CaSiO_3$ at multimegabar pressures. Proc. Natl. Acad. Sci. 108, 1252–1255.

Tsuchiya, T., Tsuchiya, J., Umemoto, K., Wentzcovitch, R.M., 2004. Phase transition in $MgSiO_3$ perovskite in the Earth's lower mantle. Earth Planet. Sci. Lett. 224, 241–248.

Umemoto, K., Wentzcovitch, R.M., 2008. Prediction of an U_2S_3-type polymorph of Al_2O_3 at 3.7 Mbar. Proc. Natl. Acad. Sci. 105, 6526–6530.

Umemoto, K., Wentzcovitch, R.M., 2010. Multi-Mbar Phase Transitions in Minerals. Rev. Mineral. Geochem. 71, 299–314.

Umemoto, K., Wentzcovitch, R.M., 2011. Two-stage dissociation in $MgSiO_3$ post-perovskite. Earth Planet. Sci. Lett. 311, 225–229.

Umemoto, K., Wentzcovitch, R.M., Allen, P.B., 2006. Dissociation of $MgSiO_3$ in the cores of gas giants and terrestrial exoplanets. Science 311, 983–986.

Unterborn, C.T., Dismukes, E.E., Panero, W.R., 2016. Scaling the Earth: a sensitivity analysis of terrestrial exoplanetary interior models. Astrophys. J. 819, 32.

Unterborn, C.T., Panero, W.R., 2017. Effects of MG/SI on exoplanetary refractory oxygen budget. arXiv:1604.08309v3 [astro-ph.EP].

Valencia, D., O'Connell, R.J., Sasselov, D., 2006. Internal structure of massive terrestrial planets. Icarus 181, 545–554.

Vanderbilt, D., 1990. Soft self-consistent pseudopotentials in a generalized eigenvalue formalism. Phys. Rev. B 41, R7892–R7895.

Wagner, F.W., Sohl, F., Hussmann, H., Grott, M., Rauer, H., 2011. Interior structure models of solid exoplanets using material laws in the infinite pressure limit. Icarus 214, 366–376.

Wallace, D., 1972. Thermodynamics of Crystals. Wiley, New York.

Wang, X., Tsuchiya, T., Hase, A., 2015. Computational support for a pyrolitic lower mantle containing ferric iron. Nat. Geosci. 8, 556.

Weinstein, S.A., 1995. The effects of a deep mantle endothermic phase change on the structure of thermal convection in silicate planets. J. Geophys. Res. 100, 11719–11728.

Weiss, L.M., Marcy, G.W., 2014. The mass-radius relation for 65 exoplanets smaller than 4 Earth radii. Astrophys. J. Lett. 783, L6.

Wentzcovitch, R.M., Karki, B.B., Cococcioni, M., de Gironcoli, S., 2004. Thermoelastic properties of $MgSiO_3$-perovskite: insights on the nature of the Earth's lower mantle. Phys. Rev. Lett. 92, 018501.

Wentzcovitch, R.M., Martins, J.L., Price, G.D., 1993. *Ab initio* molecular dynamics with variable cell shape: application to $MgSiO_3$. Phys. Rev. Lett. 70, 3947–3950.

Wright, D.J., Wittenmyer, R.A., Tinney, C.G., Bentley, J.S., Zhao, J., 2016. Three planets orbiting Wolf 1061. Astrophys. J. Lett. 817, L20.

Wu, S., Umemoto, K., Ji, M., Wang, C.Z., Ho, K.M., Wentzcovitch, R.M., 2011. Identification of post-pyrite phase transitions in SiO_2 by a genetic algorithm. Phys. Rev. B 83, 184102.

Wu, S.Q., Ji, M., Wang, C.Z., Nguyen, M.C., Zhao, X., Umemoto, K., Wentzcovitch, R.M., Ho, K.M., 2014. An adaptive genetic algorithm for crystal structure prediction. J. Phys. Condens. Matter 26, 035402.